

ELECTRONIC SUPPORTING INFORMATION

Cinnamic acid derivatives rare-earth dinuclear complexes and one-dimensionnal architectures: synthesis, characterization and magnetic properties

Ouafa Khalfaoui,^a Adel Beghidja*,^a Jérôme Long*,^b Ahlem Boussadia,^a Chahrazed Beghidja,^a Yannick Guari^b and Joulia Larionova^b

a. Unité de Recherche de Chimie de l'Environnement et Moléculaire Structurale (CHEMS), Université frères Mentouri Constantine, Route Aïn elbey, 25000 Constantine, (Algérie). E-mail: a_beghidja@yahoo.fr

b. Institut Charles Gerhardt Montpellier, UMR 5253, Ingénierie Moléculaire et Nano-Objets, Université de Montpellier, ENSCM, CNRS, Place E. Bataillon, 34095 Montpellier Cedex 5 (France). E-mail: jerome.long@umontpellier.fr

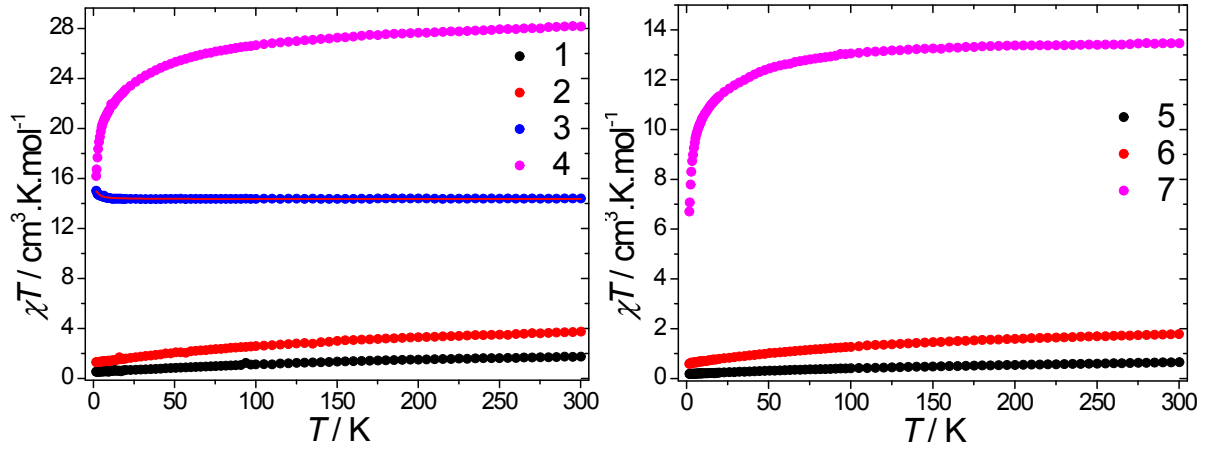


Figure S1: Left: temperature dependence of χT measured under a 1000 Oe dc field for **1-7**. The red solid lines represent the fit with the isotropic Hamiltonian.

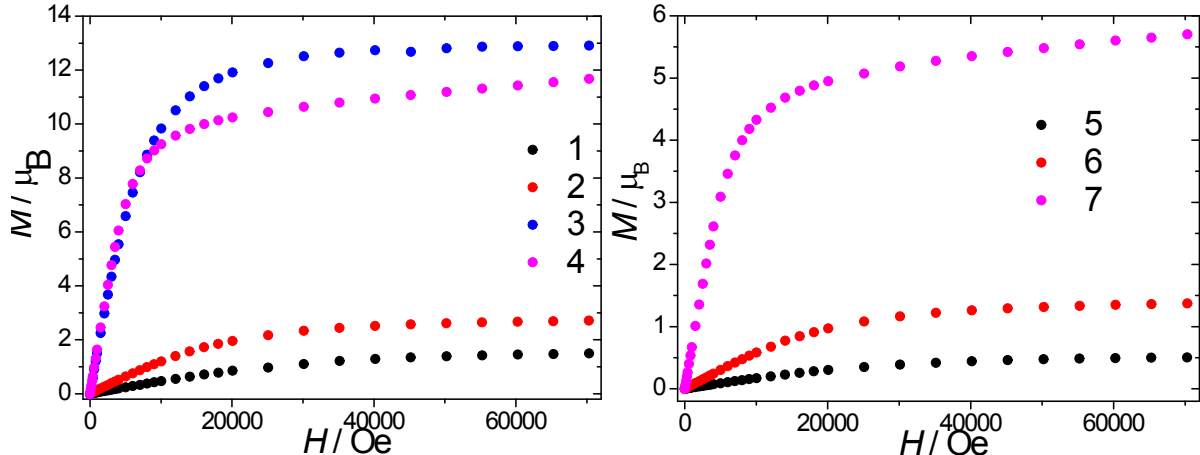


Figure S2: Field dependence of the magnetisation at 1.8 K for **1-7**.

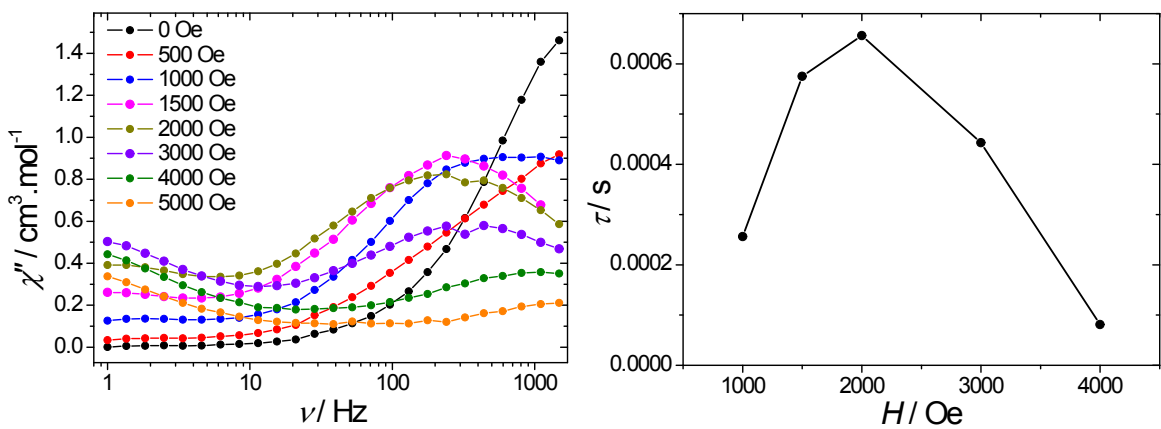


Figure S3: Left: Field dependence of the out-of-phase susceptibility, χ'' , at 1.8 K for **4**. Right: Field dependence of the relaxation time, τ , at 1.8 K for **4**.

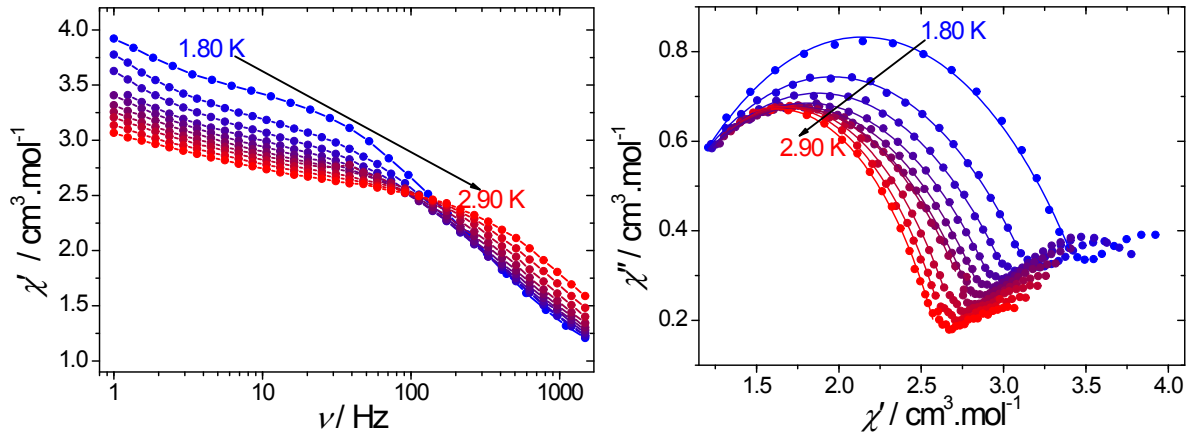


Figure S4. Left: Temperature dependence of in-phase susceptibility, χ' , measured under a 2000 Oe dc field for **4**. Right: Cole-Cole plots using the ac data performed under a 2000 Oe DC field for **4**. The solid lines correspond to the fit with a generalized Debye model.

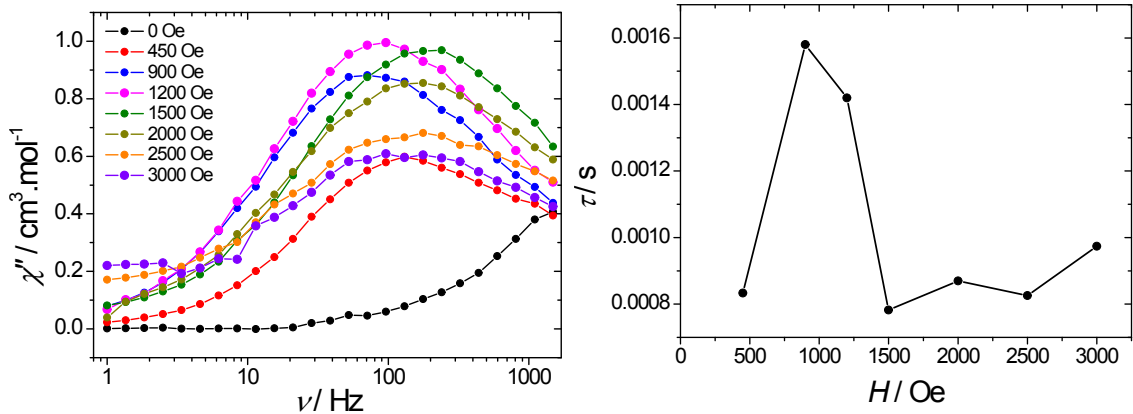


Figure S5: Left: Field dependence of the out-of-phase susceptibility, χ'' , at 1.8 K for **7**. Right: Field dependence of the relaxation time, τ , at 1.8 K for **7**.

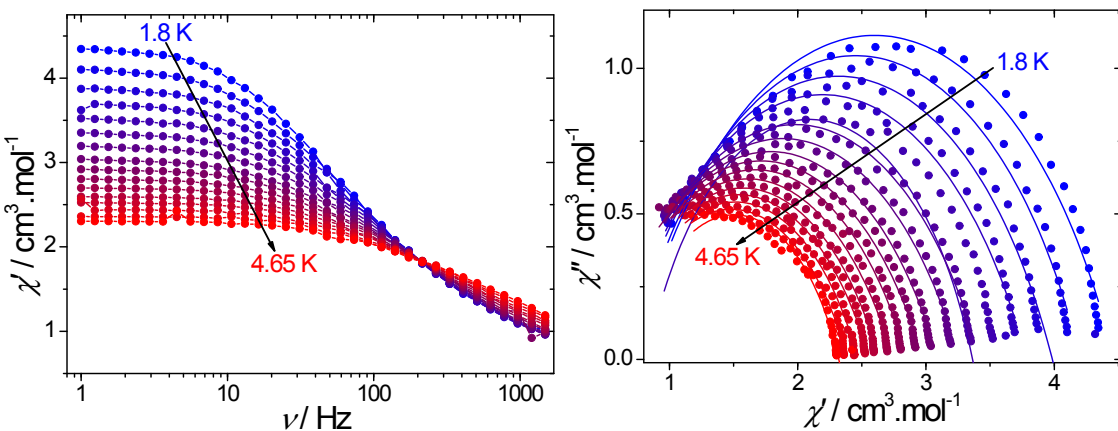


Figure S6. Left: Temperature dependence of in-phase susceptibility, χ'' , measured under a 900 Oe dc field for **7**. Right: Cole-Cole plots using the ac data performed under a 900 Oe DC field for **7**. The solid lines correspond to the fit with a generalized Debye model.

Detailed ac magnetic characterization for compound 1:

A significant out-of-phase signals were observed for **1** under a zero-dc field, but without the presence of a maximum due to a QTM (Fig. S7). However, applying dc fields shifts maximum in the frequency range available (< 1488 Hz). The optimum field which corresponds to the field for which the relaxation time, τ , is the longest is found equal to 5000 Oe (Fig. S7). The frequency dependence of the out-of-phase susceptibility for various temperatures under 5000 Oe field reveals a single frequency dependent peak indicating a field-induced slow relaxation of the magnetisation (Fig. S7). The Cole-Cole plots (Fig. S8) were fitted with a generalized Debye model, which indicate a moderate distribution of relaxation times with α parameter values ranging from 0.079 to 0.326 (Table S6). Further insights into the relaxation mechanism can be obtained through the analysis of the temperature dependence of the relaxation time (Fig. 6). As it can be seen, the absence of a clear linear part indicates a moderate contribution from a thermally activated behaviour. Attempts of fitting were performed by considering the following model: $\tau^{-1} = \tau_0^{-1} \exp(-\Delta/kT) + CT^m + AT^n$ (Eq. 1) for which the first term accounts for a thermally activated relaxation process, while the second and third ones account for Raman and direct processes respectively. To avoid over-parameterization, the values of $m = 9$ and $n = 1$ were fixed to the values found for two-phonon Raman (for Kramers ions) and direct process, although $n = 2$ can be found in the case of phonon bottleneck.^{1,2} Unfortunately, it was not possible to obtain satisfactory fitting parameters. Consequently, fitting of the temperature dependence of τ , can be performed using a model taking solely into account Raman and direct processes: $\tau^{-1} = CT^m + AT^n$ (Eq. 2) and letting the m parameter free. Reasonable fitting parameters can be obtained (Table 2). The low value of the m parameter can be imputed to the presence of acoustic phonons³ that indicates that the relaxation occurs mainly by a combination of both, Raman and direct processes.

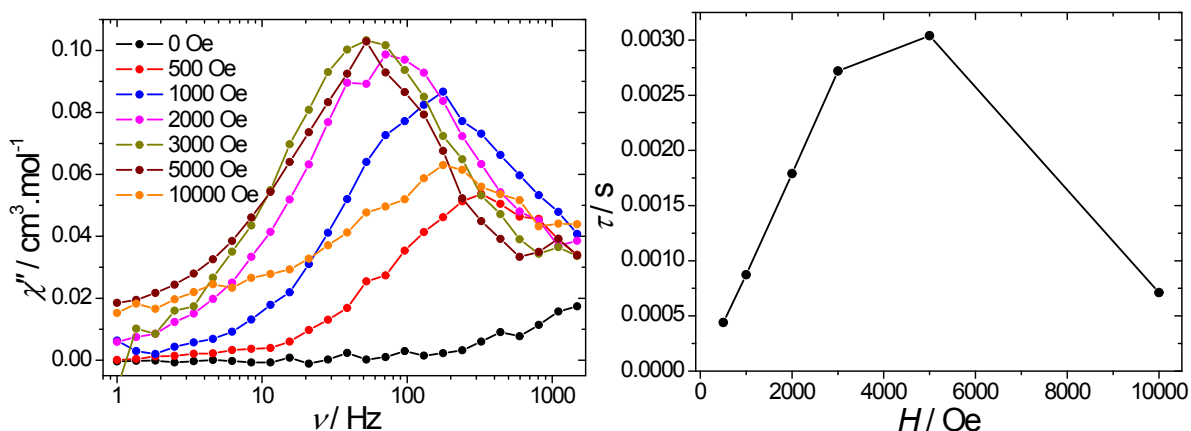


Figure S7: Left: Field dependence of the out-of-phase susceptibility, χ'' , at 1.8 K for **1**. Right: Field dependence of the relaxation time, τ , at 1.8 K for **1**.

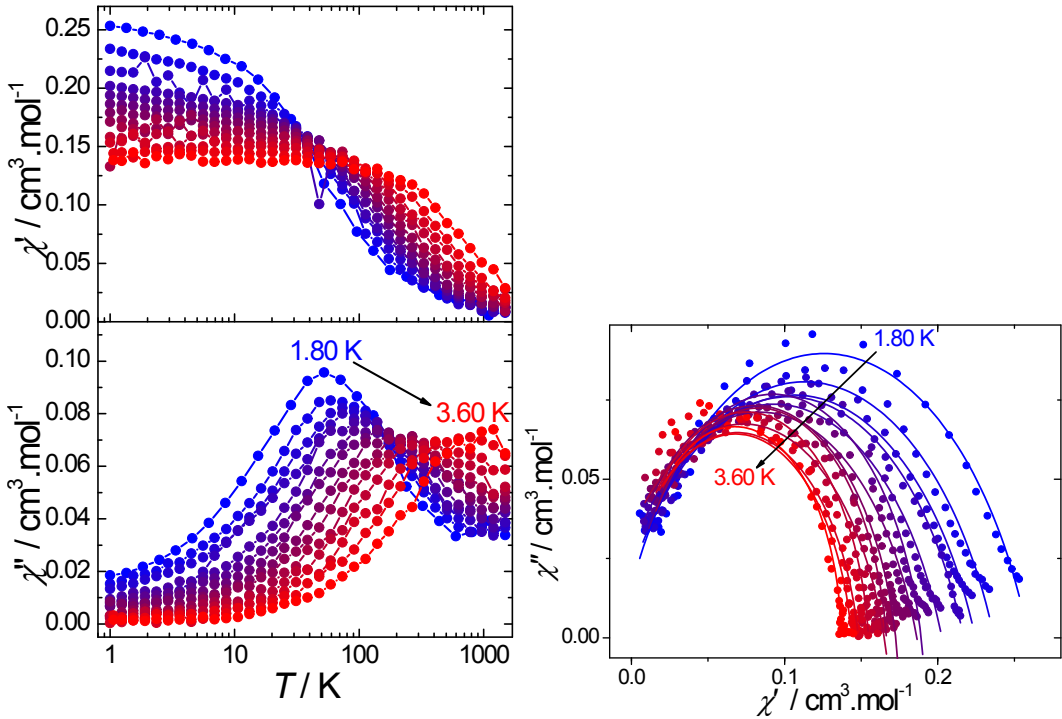


Figure S8. Left: Temperature dependence of the ac susceptibility measured under a 5000 Oe dc field for **1**. Cole-Cole plots using the ac data performed under a 5000 Oe DC field for **1**. The solid lines correspond to the fit with a generalized Debye model

Detailed ac magnetic characterization for compound 2:

Compound **2** does not show an out-of-phase component of the ac susceptibilities under a zero dc field (Fig. S9). However, applying dc fields induces the appearance of a strong out-of-phase component. The optimum field, the field for which the relaxation is the longest, is found for 2000 Oe (Fig. S9). The frequency dependence of the out-of-phase susceptibility is shown in Fig. S10 and exhibits a single peak that shifts to higher frequencies as the temperature increases confirming a slow relaxation of the magnetisation. Fitting the Cole-Cole plots with a generalized Debye model (Fig. S10) yields to moderate values of the α parameter ranging from 0.018 to 0.272, indicating a narrow distribution of the relaxations (Table S7). Fitting of the temperature dependence of the relaxation time was performed with both, Eq. 1 (Table S5) and Eq. 2 (Table 2). The low value Δ using Eq. 1 suggests a minor contribution from a thermally activated model. Fitting with Eq. 2 gives satisfactory results with $m = 5.3 \pm 0.2$, close to one of theoretical values (*i.e.* 5) expected for a Kramers ion.

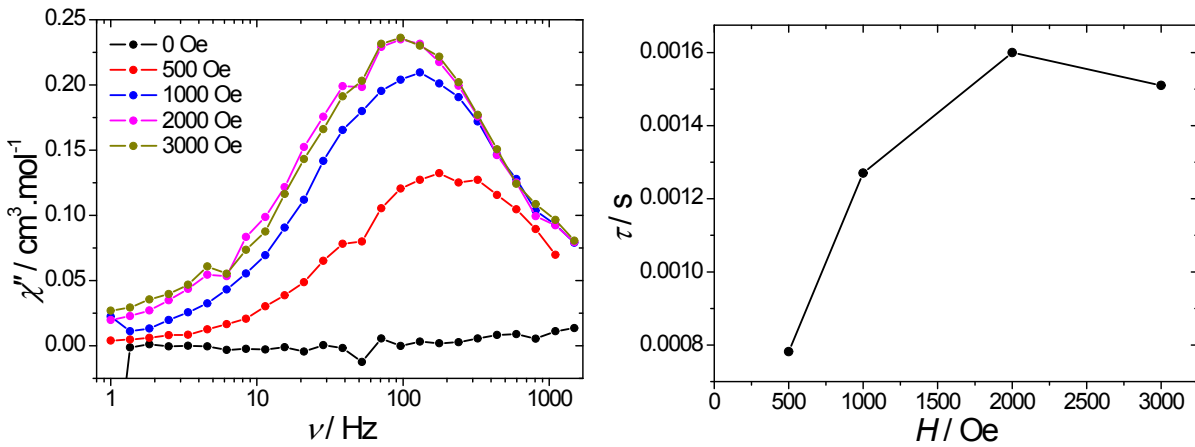


Figure S9: Left: Field dependence of the out-of-phase susceptibility, χ'' , at 1.8 K for **2**. Right: Field dependence of the relaxation time, τ , at 1.8 K for **2**.

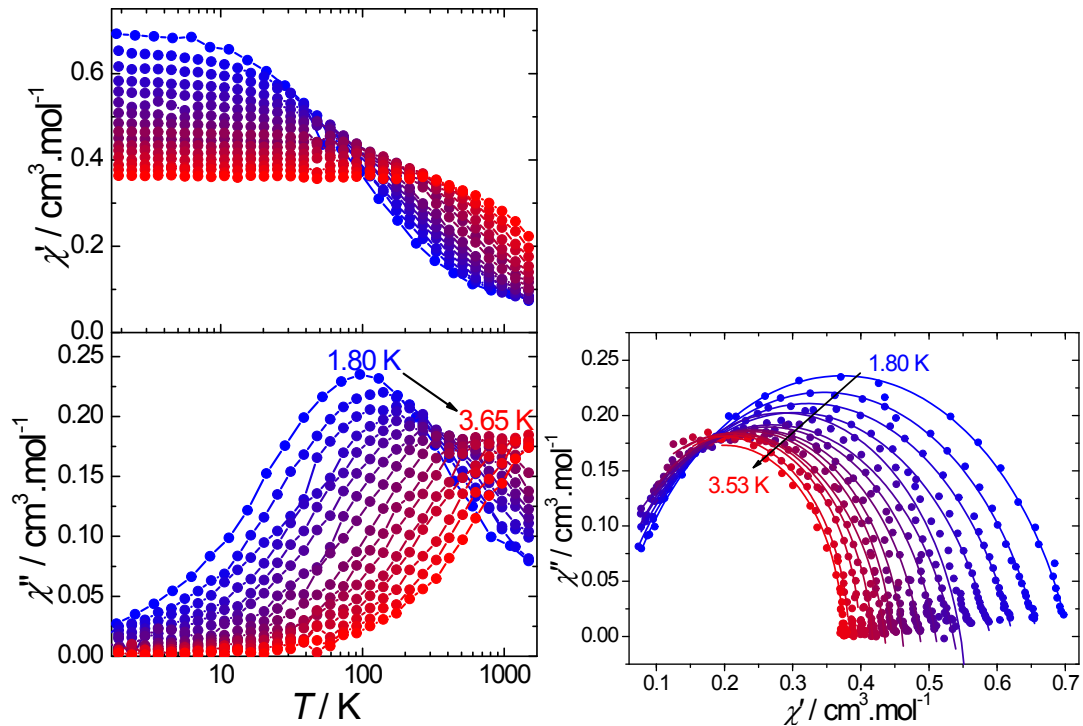


Figure S10. Left: Temperature dependence of the ac susceptibility measured under a 2000 Oe dc field for **2**. Middle: Cole-Cole plots using the ac data performed under a 2000 Oe DC field for **2**. The solid lines correspond to the fit with a generalized Debye model.

Detailed ac magnetic characterization for compound 5:

5 exhibits an out-of-phase component under a zero dc-field but without the presence of a maximum which can be revealed under the appliance of dc field (Fig. S11). The optimum field is found for 3000 Oe (Fig. S11). The frequency dependence for various temperatures performed under this field reveals the presence of a single peak (Fig. S12). However, for the highest temperatures, a plateau at high frequencies can be observed, suggesting the occurrence

of a second relaxation process which becomes evident when drawing the Cole-Cole plots (Fig. S12). The α parameter values obtained from the fitting with a generalized Debye model for the semi-circle region (ranging from 0.024 to 0.116) indicate a narrow distribution of the relaxation time for the considered process (Table S8). Unrealistic fitting parameters were obtained with Eq. 1 but the fitting of the temperature dependence of the relaxation time using Eq. 2 (Fig. 6) can be performed and indicates that the relaxation occurs mainly by a direct process and a small contribution from Raman.

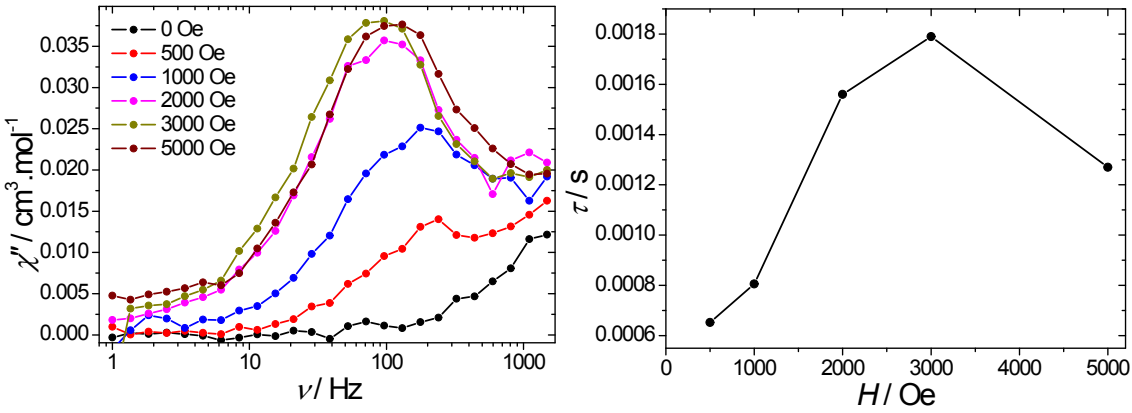


Figure S11: Left: Field dependence of the out-of-phase susceptibility, χ'' , at 1.8 K for **5**. Right: Field dependence of the relaxation time, τ , at 1.8 K for **5**.

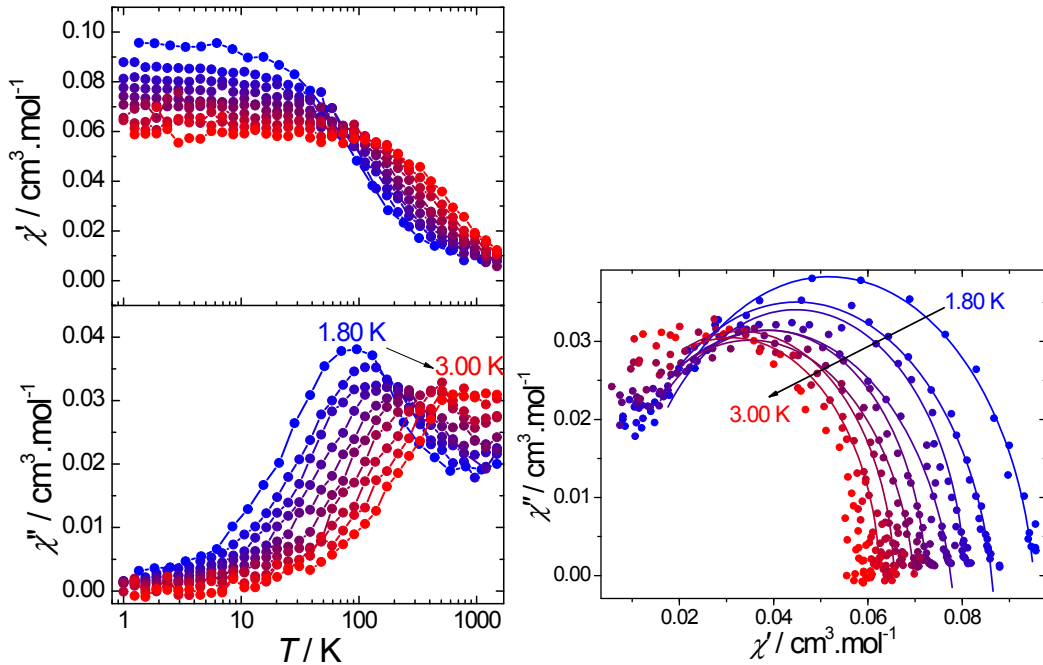


Figure S12. Left: Temperature dependence of the ac susceptibility measured under a 3000 Oe dc field for **5**. Right: Cole-Cole plots using the ac data performed under a 3000 Oe DC field for **5**. The solid lines correspond to the fit with a generalized Debye model

Detailed ac magnetic characterization for compound 6:

Compound **6** exhibits an optimum field at 2000 Oe (Fig. S13). The temperature dependence of χ'' under this optimum field reveals a single peak (Fig. S14). Fitting of the Cole-Cole plots (Fig. S14) with a generalized Debye model yields to α parameter values ranging from 0.010 to 0.260 indicating a moderate distribution of relaxation processes (Table S9). Analysis of the temperature dependence with Eq. 1 gives a small barrier of $\Delta = 8 \pm 3 \text{ cm}^{-1}$ suggesting a negligible contribution from a thermally activated process. A more reasonable fit can be obtained with Eq. 2 and gives the parameters reported in Table 1 with a m value close to the value expected for Kramers ions (*i.e.* 9). As for compound **2**, the relaxation of the magnetisation involves both Raman and direct processes.

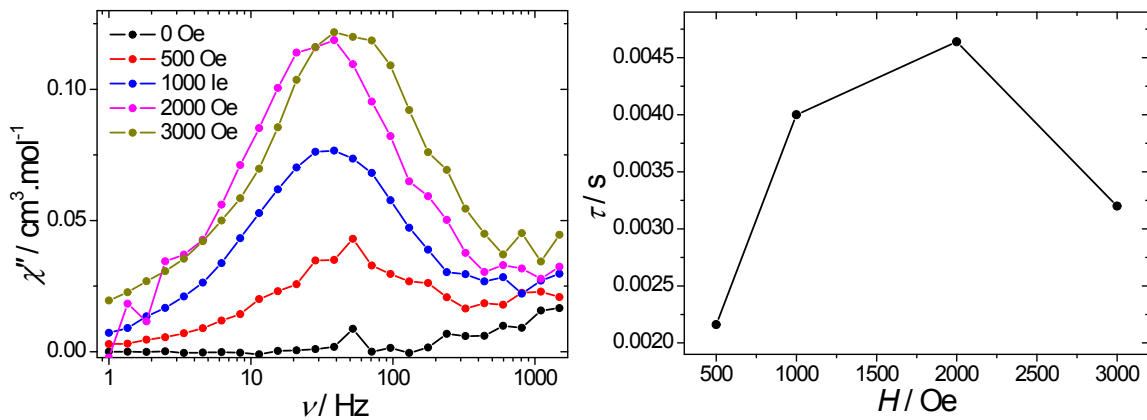


Figure S13: Left: Field dependence of the out-of-phase susceptibility, χ'' , at 1.8 K for **6**. Right: Field dependence of the relaxation time, τ , at 1.8 K for **6**.

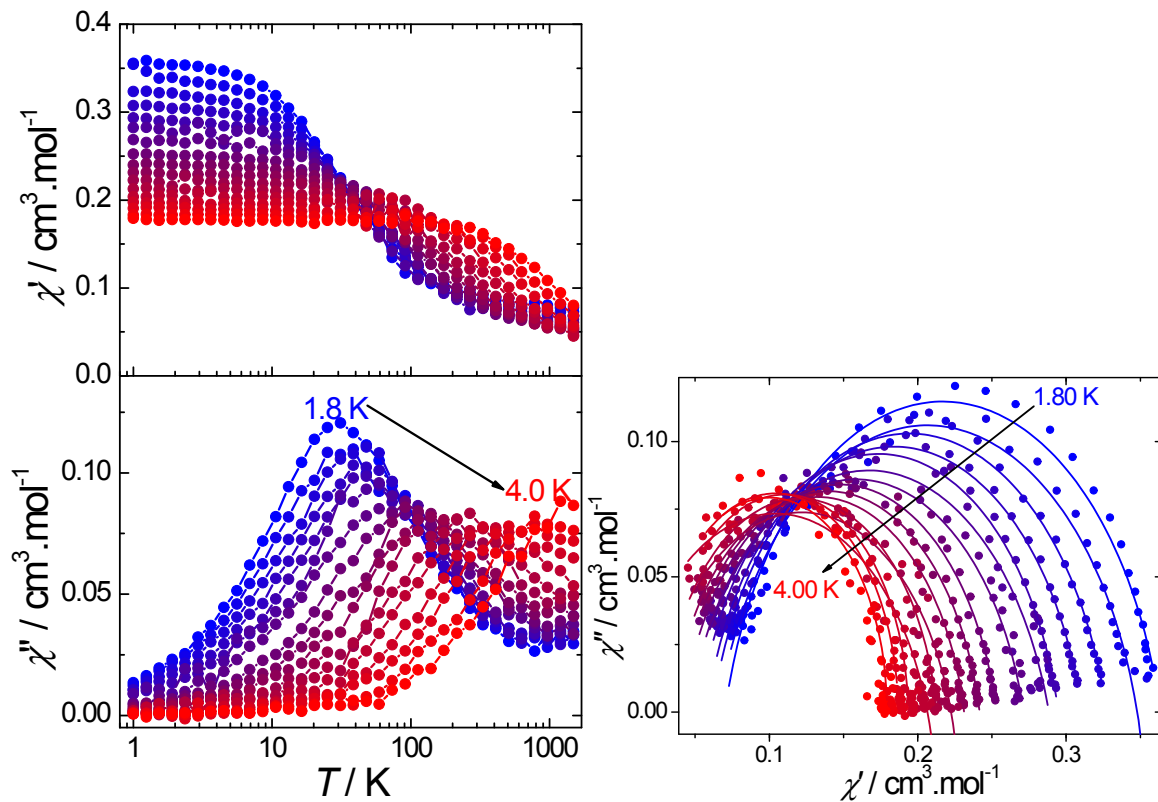


Figure S14. Left: Temperature dependence of the out-of-phase susceptibility, χ'' , measured under a 2000 Oe dc field for **6**. Right: Cole-Cole plots using the ac data performed under a 2000 Oe DC field for **6**. The solid lines correspond to the fit with a generalized Debye model

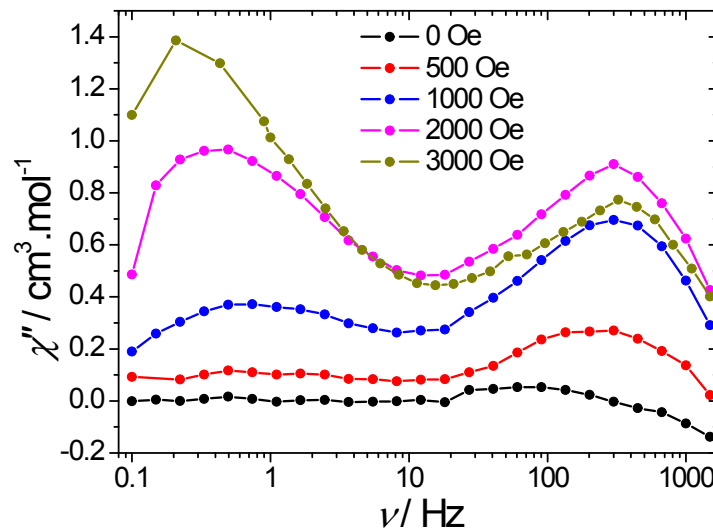


Figure S15: Field dependence of the out-of-phase susceptibility, χ'' , at 1.8 K for **3**.

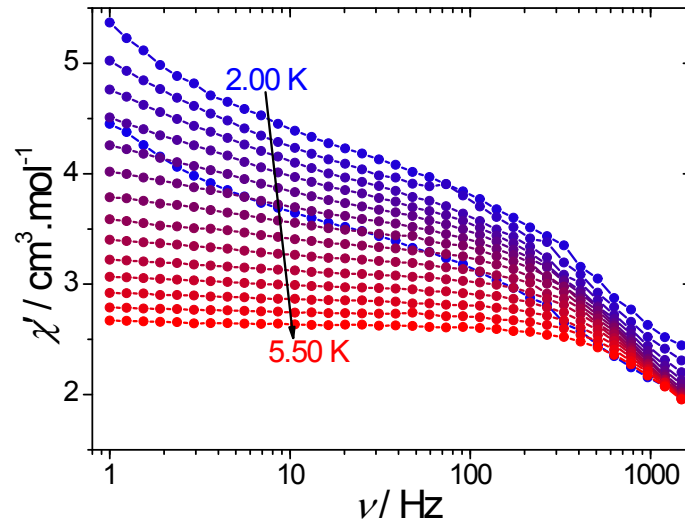


Figure S16: Temperature dependence of in-phase susceptibility, χ' , measured under a 2000 Oe dc field for **3**.

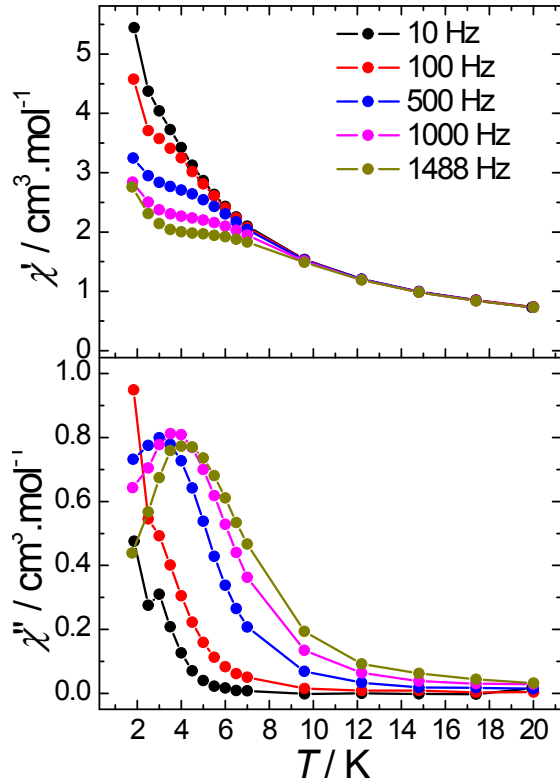


Figure S17: Temperature dependence of the ac susceptibility under a 2000 Oe dc field for **3**.

Equation used for the fitting of χT vs. T for **3:**

$$\chi_m T = \frac{2N_g^2 \beta^2}{k} \left[\frac{e^x + 5e^{3x} + 14e^{6x} + 30e^{10x} + 55e^{15x} + 91e^{21x} + 140e^{28x}}{1 + 3e^x + 5e^{3x} + 7e^{6x} + 9e^{10x} + 11e^{15x} + 13e^{21x} + 15e^{28x}} \right]$$

with $x = J/kT$

Table S1: Crystal data and experimental parameters of structures **1 - 7**

Complexes reference	1	2	3	4	5	6	7
Formula	C ₃₂ H ₂₉ CeO ₁₁ S	C ₃₂ H ₂₉ NdO ₁₁ S	C ₃₂ H ₂₉ GdO ₁₁ S	C ₃₂ H ₂₉ DyO ₁₁ S	C ₃₂ H ₃₃ CeO ₁₀ S	C ₃₂ H ₃₃ NdO ₁₀ S	C ₆₅ H ₆₈ Dy ₂ NO ₂₁ S
Mass M _w (g/mol)	761.73	765.85	778.86	784.11	749.76	753.88	1555.88
Crystal system	Monoclinic	Monoclinic	Monoclinic	Monoclinic	Triclinic	Triclinic	Triclinic
Space group	P2 ₁ /c	P2 ₁ /c	P2 ₁ /c	P2 ₁ /c	P-1	P-1	P-1
Temperature (K)	293(2)	293(2)	293(2)	293(2)	293(2)	293(2)	293(2)
a (Å)	17.4880(5)	17.474(3)	17.5136(12)	17.5183(6)	7.78230(10)	7.70450(10)	15.0687(17)
b(Å)	22.6191(6)	22.530(4)	22.5139(13)	22.4699(9)	3.4228(2)	13.4545(3)	15.4141(17)
c(Å)	8.4758(2)	8.4222(16)	8.3615(5)	8.3297(3)	16.1399(3)	16.0890(3)	16.0754(19)
α(°)	90	90	90	90	83.5470(10)	83.4560(10)	92.555(6)
γ(°)	98.9970(10)	98.658(7)	98.739(4)	98.672(2)	81.1170(10)	81.0410(10)	116.958(5)
β(°)	90	90	90	90	88.2170(10)	88.2160(10)	98.755(5)
V(Å ³)	3311.46(15)	3277.9(10)	3258.7(4)	3241.4(2)	1655.04(5)	1636.56(5)	3261.9(7)
Z	4	4	4	4	2	2	2
μcalc. (g.cm ⁻¹)	1.528	1.552	1.588	1.607	1.505	1.530	1.584
μ (mm ⁻¹)	1.495	1.705	2.157	2.428	1.492	1.704	2.380
R ₁ [I > 2σ(I)]	0.0456	0.0433	0.0834	0.0494	0.027	0.023	0.0392
wR ₂ [I > 2σ(I)]	0.0900	0.0805	0.1501	0.0839	0.0614	0.052	0.0910
GOF (F ²)	1.323	1.067	1.205	1.258	1.046	1.04	1.018
Residual electron density, e Å ⁻³ (ρ _{min} /ρ _{max})	1.41/-0.83	1.28/-0.67	1.12/-1.03	0.98/-0.80	1.74/-0.68	0.89/-0.45	2.34/-1.80

$$^a R1 = \sum |F_o| - |F_c| / \sum |F_o|; ^b wR2 = \sqrt{\sum [w(F_o^2 - F_c^2)^2] / \sum [w(F_o^2)^2]}$$

Table S2. SHAPE analysis.

JJCU	CCU	JCSAPR	CSAPR	JTCTPR	TCTPR
------	-----	--------	-------	--------	-------

1	10.736	9.154	3.592	2.625	4.533	3.768
2	10.663	9.062	3.426	2.497	4.242	3.568
3	10.283	8.801	3.221	2.332	3.706	3.183
4	10.193	8.797	3.103	2.296	3.407	3.058
5	9.622	8.692	4.183	3.191	5.756	3.529
6	9.533	8.626	4.134	3.151	5.722	3.469
7 Dy1	10.264	9.043	2.830	2.209	2.817	2.530
7 Dy2	9.861	9.254	2.296	1.742	3.012	2.094

JJCU:Capped cube

CCU: Spherical-relaxed capped cube

JCSAPR: Capped square antiprism

CSAPR: Spherical capped square antiprism

JTCTPR: Tricapped trigonal prism

TCTPR: Spherical tricapped trigonal prism

Table S3. Fitting of the Cole-Cole plots with a generalized Debye model for temperature ranging from 1.8 to 2.90 K under a 2000 Oe DC field for **4**.

T (K)	α	χ_s (cm ³ . mol ⁻¹)	χ_T (cm ³ . mol ⁻¹)
1.80	0.629	1.436	2.849
2.00	0.737	1.469	2.447
2.10	0.770	1.460	2.290
2.21	0.789	1.435	2.180
2.33	0.706	1.283	2.255
2.44	0.655	1.182	2.271
2.55	0.597	1.122	2.328
2.67	0.465	1.000	2.389
2.78	0.425	0.939	2.364
2.90	0.396	0.909	2.340

Table S4. Fitting of the Cole-Cole plots with a generalized Debye model for temperature ranging from 1.8 to 2.90 K under a 2000 Oe DC field for **7**.

T (K)	α	χ_s (cm ³ . mol ⁻¹)	χ_T (cm ³ . mol ⁻¹)
1.80	0.459	1.450	3.747
2.00	0.469	1.376	3.527
2.20	0.487	1.332	3.299

2.40	0.510	1.294	3.097
2.60	0.359	1.205	2.983
2.80	0.541	1.206	2.756
3.00	0.562	1.172	2.596
3.20	0.576	1.131	2.444
3.40	0.593	1.102	2.328
3.60	0.565	1.061	2.280
3.80	0.575	1.039	2.182
4.00	0.560	1.017	2.123
4.15	0.557	1.002	2.069
4.30	0.523	0.986	2.045
4.50	0.520	0.975	1.987
4.65	0.432	0.984	2.025

Table S5. Fit parameters of the relaxation time obtained with Eq. 1.

Compound	Δ (cm ⁻¹)	τ_0 (S)	C (s ⁻¹ .K ⁻⁹)	A (s ⁻¹ .K ⁻¹)
1 (5000 Oe)	-	-	-	-
2 (2000 Oe)	12 ± 2	$(1.2 \pm 0.7) \times 10^{-6}$	0.01 ± 0.01	337 ± 32
4 (2000 Oe)	2.2 ± 0.9	$(1.0 \pm 0.5) \times 10^{-4}$	0.36 ± 0.03	0
6 (2000 Oe)	8 ± 3	$(6 \pm 7) \times 10^{-5}$	0.024 ± 0.001	102 ± 26
7 (900 Oe)	9.5 ± 0.9	$(2.4 \pm 0.8) \times 10^{-5}$	0.0012 ± 0.002	262 ± 13

Table S6. Fitting of the Cole-Cole plots with a generalized Debye model for temperature ranging from 1.80 to 3.60 K under a 5000 Oe DC field for **1**.

T (K)	α	χ_s (cm ³ . mol ⁻¹)	χ_T (cm ³ . mol ⁻¹)
1.80	0.326	0.028	0.223
2.00	0.356	0.026	0.200
2.125	0.362	0.024	0.188
2.250	0.335	0.020	0.185
2.375	0.320	0.013	0.173
2.50	0.168	0.010	0.175
2.625	0.289	0.006	0.161
2.75	0.165	0.002	0.159
2.875	0.100	0.006	0.159

3.00	0.237	0.000	0.237
3.125	0.079	0.000	0.149
3.25	0.146	0.000	0.138
3.40	0.118	0.000	0.136
3.60	0.029	0.000	0.135

Table S7. Fitting of the Cole-Cole plots with a generalized Debye model for temperature ranging from 1.80 to 3.53 K under a 2000 Oe DC field for **2**.

T (K)	α	χ_s (cm ³ . mol ⁻¹)	χ_T (cm ³ . mol ⁻¹)
1.80	0.272	0.115	0.629
1.95	0.279	0.104	0.585
2.07	0.279	0.094	0.553
2.19	0.273	0.083	0.524
2.31	0.187	0.068	0.504
2.43	0.254	0.061	0.478
2.55	0.195	0.059	0.468
2.68	0.173	0.049	0.451
2.80	0.115	0.043	0.438
2.92	0.086	0.041	0.429
3.04	0.129	0.019	0.410
3.16	0.070	0.022	0.403
3.28	0.013	0.029	0.394
3.40	0.018	0.013	0.379
3.53	0.001	0.028	0.373

Table S8. Fitting of the Cole-Cole plots with a generalized Debye model for temperature ranging from 1.8 to 2.75 K under a 3000 Oe DC field for **5**.

T (K)	α	χ_s (cm ³ . mol ⁻¹)	χ_T (cm ³ . mol ⁻¹)
1.80	0.089	0.011	0.091
2.00	0.116	0.008	0.082
2.125	0.032	0.010	0.079

2.25	0.072	0.005	0.072
2.375	0.041	0.006	0.071
2.50	0.096	0.003	0.066
2.625	0.025	0.0013	0.064
2.75	0.024	0.000	0.061

Table S9. Fitting of the Cole-Cole plots with a generalized Debye model for temperature ranging from 1.8 to 2.90 K under a 2000 Oe DC field for **6**.

T (K)	α	χ_s (cm ³ . mol ⁻¹)	χ_T (cm ³ . mol ⁻¹)
1.80	0.141	0.093	0.341
1.92	0.219	0.091	0.321
2.04	0.191	0.083	0.305
2.16	0.190	0.078	0.290
2.28	0.175	0.071	0.276
2.40	0.236	0.070	0.264
2.52	0.204	0.065	0.251
2.70	0.167	0.057	0.238
2.85	0.162	0.052	0.227
3.00	0.156	0.047	0.218
3.13	0.238	0.041	0.202
3.28	0.108	0.038	0.203
3.42	0.260	0.024	0.184
3.56	0.023	0.028	0.191
3.71	0.015	0.022	0.185
3.85	0.010	0.021	0.179

- 2 P. L. Scott and C. D. Jeffries, *Phys. Rev.*, 1962, **127**, 32.
3 S. T. Liddle and J. van Slageren, *Chem. Soc. Rev.*, 2015, **44**, 6655.